LA-UR-16-23338

Title:	All-Particle Spontaneous-Decay and Delayed-Positron Capabilities in MCNP6
Author(s):	Tutt, James Robert Mckinney, Gregg Walter Wilcox, Trevor
Intended for:	Advances in Nuclear Nonproliferation Technology and Policy Conference (ANTPC), 2016-09-25/2016-09-30 (Santa Fe, New Mexico, United States)
Issued:	2016-05-26 (rev.1)

All-Particle Spontaneous-Decay and Delayed-Positron Capabilities in MCNP6

J. R. Tutt, G.W. McKinney, T. A. Wilcox

Los Alamos National Laboratory, Bikini Atoll Rd. P.O. Box 1663, MS-C921, Los Alamos, NM 87545
jtutt@lanl.gov, gwm@lanl.gov, wilcox@lanl.gov

INTRODUCTION

Delayed-particle signatures have important applications in areas such as nuclear safeguards and forensics, medical physics, and the design of radiation instrumentation, to name a few. As a result, there has been a continued interest in computational tools for delayed-particle simulation. To address this interest, in 2005, a delayed-particle physics package was developed for the Monte Carlo radiation transport code MCNPX [1] through the incorporation of the CINDER90 [2] depletion code. This capability allowed the simulation of delayed-neutron and delayed-gamma radiation from spontaneous decay, activation, or unstable residuals from fission reactions [3]. MCNP6 [4] inherited this delayed-particle production capability when it was created through the merger of MCNP5 [5] and MCNPX in 2010. Since then, the delayed particle capability in MCNP6 has been the subject of continuous improvement, through algorithm enhancements [6,7], expansion of particle types to delayed-electron and delayed-alpha particles [6,8], and library improvements [9].

The most recent updates to the delayed-particle feature in MCNP6 include the addition of ENDF/B-VII.1 [10] delayed-positron data to delay_library.dat_v5, along with a delayed-positron source capability, and an all-particle spontaneous-decay source option, which are the subjects of this paper. In addition to descriptions of these updates, several examples are presented to show their functionality and results from the delayed-positron examples are compared against measured data.

ALL-PARTICLE SPONTANEOUS-DECAY SOURCE OPTION

The all-particle spontaneous-decay source (SD) option has been added to the source particle type (PAR) keyword to more easily allow production of all possible spontaneous particles in a given problem. Placing PAR=SD on the source definition (SDEF) card is equivalent to selecting all spontaneous-decay types, which could otherwise only be accomplished with a source distribution. This allows more straight forward normalization (simply the activity in Bq) for the spontaneous-decay source and reduces the overall number of histories when multiple spontaneous-decay particle sources are used. When using the PAR=SD option, the only way to turn off production of a particle type is to omit that particle from the MODE card.

DELAYED-POSITRON CAPABILITY

The delayed-positron capability allows a user to simulate positrons emitted spontaneously from unstable radionuclides. To accommodate this feature, ENDF/B-VII.1 positron emission data has been included in the delay_library.dat Version 5 data file. Positron spectral data is now represented for 531 radionuclides in a bin-wise format consisting of 100 equally spaced energy bins from 0 to 10 MeV.

Invoking delayed-positrons from spontaneous radionuclide decay is accomplished on the SDEF card by setting PAR keyword equal to either the spontaneous positron particle designator (ST) or to the nuclide identification number (ZZAAA) of a positron-emitting radionuclide. Delayed-positrons from activation, fission, or spontaneous decay residuals can be enabled on the activation control (ACT) card by including the positron particle designator (F) on the non-fission residual (NONFISS) and/or the fission residual (FISSION) keywords.

Several considerations should be taken into account when transporting and/or tallying on positrons in MCNP6. First, in MCNP6, positron and electron physics are treated identically except in certain instances such as tracking directions in magnetic fields and in the treatment of positron annihilation. For this reason, enabling electron transport on the MODE card also enables positron transport ('F' is not currently a legal entry on the MODE card). Similarly, tallying on positrons requires an electron tally specification card (Fn:E) and the use of a special treatment for tallies card (FTn) with the electron current tally (ELC) keyword. The ELC keyword has one parameter, c, that can be used to specify how the charge of a particle effects a tally and/or separate positron and electron tallies (c=1 causes negative scores from negatively charged particles, c=2 splits charged particles and antiparticles into separate user bins, c=3 combines the functionality of c=1 and c=2). Additionally, in electron transport the default electron energy cutoff is 1 keV (and can be explicitly lowered to 10 eV). Electrons below this cutoff are eliminated, while positrons below the energy cutoff produce annihilation photons.

RESULTS

To show the functionality of the all-particle spontaneous-decay source option, an example problem was created in which a 0.001 radius sphere of U-238 decays. The PAR=SD option was used to enable spontaneous alpha, beta,

and gamma decay source particles which were volumetrically distributed throughout the sphere. The activity of the uranium sphere was obtained from the material activities table (Print Table 44) in the MCNP output file and found to be 9.983×10^{-4} Bq. This activity was then used on the particle weight keyword (WGT) to normalize each source particle with the activity of the U-238 sphere. The alpha, beta, and gamma spectra of U-238 and its daughters (assuming equilibrium decay) obtained from this simulation is shown in figure 1 with integral values for each particle type provided in the legend. The alpha spectrum is continuous due to MCNP's use of the continuous-slowing-down approximation (CSDA) and has a maximum at ~7.7 MeV (Po-214) with peaks corresponding to other prominent alpha-emitters in the U-238 decay chain. As expected, the beta spectrum is also continuous with a maximum at ~3.2 MeV (Bi-214) while the gamma spectrum, sampled from line data using DG=LINES on the ACT card, appears in discrete energy lines.
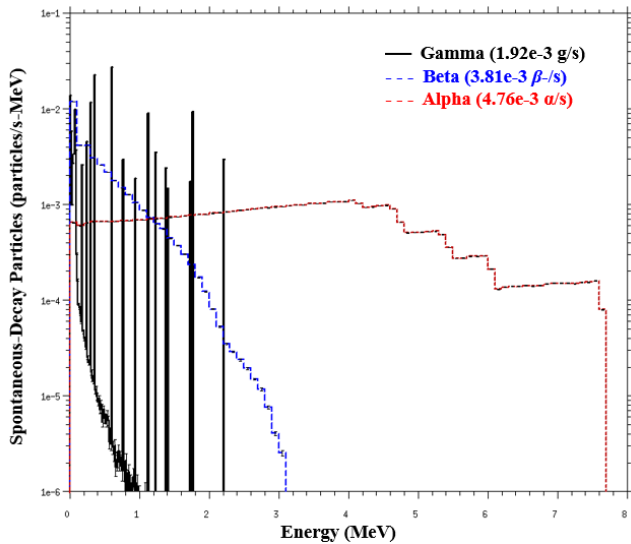

Fig. 1 – MCNP6 simulated alpha, beta, and gamma decay spectra of U-238 and daughters (assuming equilibrium decay) using PAR=SD source.

Several more examples have been created to demonstrate the delayed-positron capability and verify its accuracy. In the first example, the delayed-particle spectra from a Cu-64 spontaneous decay source was examined. The decay of Cu-64 emits both delayed-electrons and delayed-positrons and therefore demonstrates well the delayed-particle simulation capability of MCNP6. The input deck for this case consists of a Cu-64 sphere with a radius of 1 cm. A source distribution (Dn) is specified on the PAR keyword and spontaneous electrons (SB) and spontaneous positrons (ST) are listed with the 'L' option (denoting discrete values) on the source information card (SIn) and given equal weights on the source probability card (SPn). The data cards for this source are shown here,

```
MODE E
M1    29064 1
SDEF PAR=D1
SI1   L SB ST
SP1      1  1
```

The LCA 7j -2 option was employed to immediately transport all secondary particles to the problem boundaries without further interactions. This ensures that electrons and positrons created from spontaneous decay anywhere within the sphere are allowed to exit the surface and can be scored using a surface current (F1) tally. The tally cards for this case are as follows,

```
F1:E 1
FT1   ELC 2
E1    0 99i 10.0
```

where, the F1 tally accumulates electron/positron current crossing surface 1 (1cm sphere described above). Note that 'E' is the required particle designator on the F1 tally. Placing the 'F' positron particle designator on a tally is not currently allowed and will result in a fatal error. As discussed earlier, the FT card with ELC keyword was used with option 2 to separate electron and positron tallies into separate user bins. Finally, the tally energy card, E1, divides the tally into 100 equally spaced energy bins between 0 and 10 MeV, matching the bin structure of electron and positron data in delay_library_v5.dat which is the energy resolution limit (more bins would simply result in a stair-step structure in the tally spectrum). The results, shown in figure 2, have been converted from MeV to momentum and scaled to the maximum measured curve height for comparison with experimental data published by Cook et al. [11]. The electron and positron spectra produced with MCNP6 shows good agreement with the experimental data with the exception of a large peak in the electron spectrum between 0.0 and 0.8 p/mc which is caused by Cu-64 K and L Auger electron emissions included in the first 100 keV energy bin of the ENDF data.
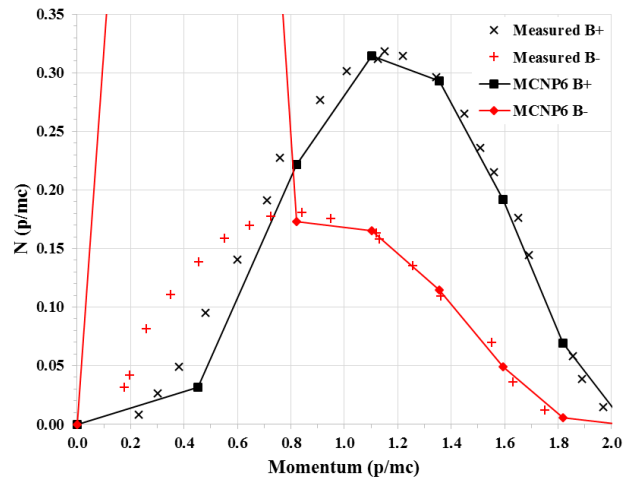

Fig. 2 – MCNP6 simulated electron and positron spectra from β +/- decay of Cu-64 compared to measured data.

The second example shows delayed-positrons emitted from activation residuals through the use of the NONFISS keyword on the ACT card. For this example, a simple model was created to simulate the physics of accelerator-production of F-18 from proton activation of O-18. To form this model, 15 MeV protons are incident on an O-18 target. The LCA 7j -2 option was again used to force the protons to immediately collide with the O-18 nuclei and allow any secondary radiations from the interaction escape. Proton-neutron (p,n) reactions on the O-18 nuclei create F-18 residuals (and a small amount of F-17 residuals via (p,2n) reactions). The NONFISS=f keyword was used on the ACT keyword to enable delayed positron emission from the F-18 residuals. A positron surface current tally was set up as in the first example and the results, shown in figure 3, were scaled to the maximum measured intensity for comparison with a F-18 positron spectrum published by A. Crespo [12], showing good agreement.

In the third example, a simple Ge-68/Ga-68 generator, in which Ge-68 decays via electron capture to the positron emitter Ga-68, is modeled. The geometry for this model consisted of a 1cm-radius sphere filled with void. A Ge-68 radionuclide source was placed at the center of the sphere by setting PAR=32068, the ZZAAA number for Ge-68, and ERG=0. As the Ge-68 source decayed, it produced Ga-68 residuals which in turn emitted delayed-positrons when NONFISS=f was invoked. The tallied results are shown in figure 3, scaled to maximum measured intensity, and compared to the positron spectra from Ga-68 found in A. Crespo [12].
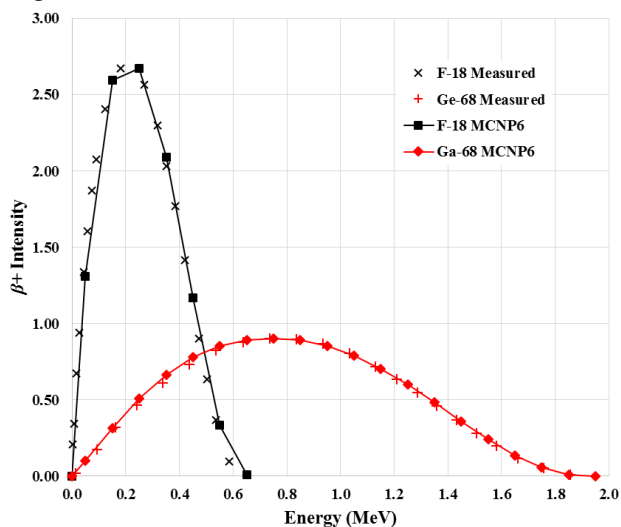

Fig. 3 – MCNP6 simulated positron spectra from β + decay of F-18 and Ga-68 compared to measured data.

CONCLUSION

Improvements have been made to the delayed-particle capability in MCNP that include a delayed-positron source capability which samples ENDF/B-VII.1 positron emission data for 531 available radionuclides and an all-particle spontaneous-decay source option that enables convenient sampling of all delayed-particle types. Several examples have been provided and discussed to demonstrate these new capabilities. Furthermore, the results of the delayed-positron examples have been compared with measured data to show validity. These capabilities will be available in the MCNP 6.2.0 release in 2016.

ENDNOTES

REFERENCES

1. D. B. Pelowitz, editor, "MCNPX User's Manual, Version 2.5.0," Los Alamos National Laboratory Report LA-CP-05-0369 (2005).
2. W. Wilson, T. England, D. George, D. Muir, and P. Young, "Recent Development of the CINDER90 Transmutation Code and Data Library for Actinide Transmutation Studies," Los Alamos National Laboratory Report LA-UR-95-2181 (1995).
3. J. W. Durkee, M. R. James, G. W. McKinney, L. S. Waters, J. T. Goorley, "The MCNP6 Delayed-Particle Feature, LA-UR-11-05379, *Journal of Nuclear Technology* (2011).
4. D. B. Pelowitz, A.J. Fallgren, and G.E. McMath, editors, "MCNP6 User's Manual, Version 6.1.1beta," LANL report LA-CP-14-00745 (2014).
5. F. Brown et al., "MCNP - A General Monte Carlo N-Particle Transport Code, Version 5 - Volume 1 Overview and Theory," Los Alamos National Laboratory Report LA-CP-03-1987 (2003).
6. G. W. McKinney, "MCNP6 Enhancements of Delayed-Particle Production, LA-UR-11-06426, PHYSOR 2012, Knoxville, TN, April 15-20, (2012).
7. J. R. Tutt, G. W. McKinney, T. A. Wilcox, G. E. McMath, "MCNP 6.2.0 Delayed-Particle Production Improvements," LA-UR-15-29614, Proceedings of the ANS Summer Meeting, New Orleans, LA, June 12-16 (2016).
8. G. E. McMath, G. W. McKinney, "Proceedings of the ANS Summer Meeting," Proceedings of the ANS Winter Meeting, Anaheim, CA, November 9-13 (2014).
9. T. A. Wilcox, G. W. McKinney, "MCNP Delayed-Particle Library – Release 5," Proceedings of the ANS Winter Meeting, Washington, DC, November 8-12 (2015).
10. M. B. Chadwick, et al., "ENDF/B-VII.1: Nuclear Data for Science and Technology: Cross Sections,

Covariances, Fission Product Yields and Decay Data," *Nucl. Data Sheets*, **112**, 2887 (2011).

11. C. S. Cook, L. M. Langer, "The Beta Spectrum of Cu64 as a Test of the Fermi Theory," *Physical Review*, **73**, No. 6, 601 (1947).

12. A. Sanchez-Crespo, "Comparison of Gallium-68 and Fluorine-18 imaging characteristics in positron emission tomography," *Applied Radiation and Isotopes*, **76**, 55-62 (2013).